

Effects of *Albizia julibrissin* Durazz through Suppression of Mitochondrial Fission and Apoptosis in Cisplatin-induced Acute Kidney Injury

Hui-Ju Lee¹, Kyung-Hyun Kim¹, Yae-Ji Kim¹, Sung-Pil Cho¹, Geum-Lan Hong², and Ju-Young Jung^{1,*}

¹Department of Veterinary Medicine & Institute of Veterinary Science, Chungnam National University, Daejeon 34134, Republic of Korea

²Department of Anatomy, College of Medicine, Konyang University, Daejeon 35365, Republic of Korea

Abstract – *Albizia julibrissin* Durazz. (AJ; family Mimosaceae) is widely distributed worldwide, and its stem bark has been used as a traditional herbal medicine. Acute kidney injury (AKI) is a clinical syndrome that results in sudden loss of renal function. This study aimed to investigate the effects of AJ against cisplatin-induced AKI using a human kidney proximal tubule epithelial cell line (HK-2) and cisplatin-treated mice. *In vitro*, cisplatin treatment increased apoptosis in HK-2 cells. However, AJ treatment decreased apoptosis of cisplatin-treated HK-2 cells. *In vivo*, cisplatin treatment accelerated renal injury by increasing the levels of renal injury markers, such as blood urea nitrogen, creatinine, kidney injury molecule 1, and neutrophil gelatinase-associated lipocalin, which were reversed by AJ treatment. Histopathologically, AJ treatment resulted in decreased renal damage with less tubular necrosis and brush border desquamation compared with the AKI group. Additionally, cisplatin treatment upregulated mitochondrial fission, a pathological characteristic of AKI, which was downregulated by AJ treatment. Along with increased mitochondrial fission, AJ treatment also reduced cisplatin-induced apoptosis. These results suggest that AJ may be a potential therapeutic agent for cisplatin-induced AKI.

Keywords – Acute kidney injury, *Albizia julibrissin* Durazz, apoptosis, mitochondrial fission

Introduction

Albizia julibrissin Durazz. (AJ; family Mimosaceae), known as the Persian silk tree, is widely distributed in East Asia, mid-Asia, Africa, and North America.¹⁻² The flowers and bark of AJ are medicinally used as traditional herbal medicines to alleviate insomnia,³ melancholia, hemorrhoids, bruises, and ulcers⁴ in East Asia. Recently, a variety of pharmaceutical effects of AJ have been reported including anti-tumor,⁵ neuroprotective,⁶ and anti-inflammatory⁷ properties. Several reports have shown that AJ extract contains flavonol glycosides, triterpenoids, quercitrin, and saponins.⁵⁻⁶

Acute kidney injury (AKI) is a clinical syndrome that results in the sudden loss of renal function within a few hours or days. It commonly occurs in 10-15% of hospitalized patients in the intensive care unit, with a high mortality rate of up to 50%. The development of AKI is associated with various etiologies, including sepsis, renal

ischemia-reperfusion, and nephrotoxins.⁸ In particular, the toxic effects of various chemical drugs entering the body are a major target for the kidneys, and drug-induced AKI frequently occurs in clinical medicine. Cis-diammine-dichloroplatinumII (cisplatin) is a platinum containing chemotherapeutic agent that has been widely used to treat diverse solid malignant tumors such as testis, bladder, ovarian, colorectal, and lung cancers.⁹⁻¹⁰ However, the use of cisplatin is limited owing to critical side effects. Notably, the most highlighted side effect is nephrotoxicity. Cisplatin exhibits high reactivity within cells and causes DNA damage. The molecular transporters in the renal proximal tubular cells mediates the cellular uptake of cisplatin, resulting in the accumulation of cisplatin in renal proximal tubular cells.¹¹ In particular, the renal proximal tubule is characterized by a higher mitochondrial content than other renal cells to meet the enormous energy demands for reabsorption and secretion of kidney.⁹ In this regards, the proper morphological structure of mitochondria is essential to maintain homeostasis in the renal proximal tubule, and it is affected by the balance between mitochondrial fission (mitochondria are separated into two) and fusion (two mitochondria are combined into

*Author for correspondence

Ju-Young Jung, DVM, PhD, College of Veterinary Medicine, Chungnam National University, 220 Gung-dong, Yuseong-gu, Daejeon 34134, Republic of Korea.

Tel: +82-42-821-8899,7902; E-mail: jyjung@cnu.ac.kr

one).¹² At the basal level, fission plays an important role in isolating damaged mitochondria and leads to the clearance of dysfunctional mitochondria.¹³ However, excessive fission, induced by accumulated cisplatin results in mitochondrial fragmentation, resulting in the release of pro-apoptotic factors. In this regard, an imbalance between fission and fusion is associated with the progression of cell death during AKI.¹⁴ Cisplatin-induced AKI ultimately leads to renal proximal tubular injury and renal function deterioration.¹⁵ After cisplatin-induced AKI, the remaining renal tubular cells undergo a series of repair systems such as dedifferentiation, proliferation, and immigration.¹⁶ However, severe and sustained renal injury can lead to chronic kidney disease, making restoration impossible. Although the fatality rate of AKI continues to increase, there are no distinct interventions to treat or prevent AKI.¹⁷ In this regard, there is an emerging need for agents for AKI treatment and mitigation.

Various pharmacological effects of AJ have been reported.⁵⁻⁷ However, the effect of AJ on cisplatin-induced AKI has not been elucidated. This study aimed to examine the effects of AJ on cisplatin-induced AKI using *in vitro* and *in vivo* models.

Experimental

Plant material and extract preparation – The name of the plant, *Albizia julibrissin* Durazz., was verified at Plants of the World Online (<http://www.plantsoftheworldonline.org/>). The plant samples used in this study were purchased from Dongkyoung General Trading Company (Dandong, China) and obtained from Prof. Gyu-Yong Song, College of Medicine, Chungnam National University (Daejeon, Korea). The AJ extract (20 g) was prepared according to the aforementioned conditions¹⁸. The AJ material was ground and extracted in 300 mL of methanol at 40°C for 3 h by sonication. The AJ solution was filtered through filter paper, and the residue was extracted in 300 mL of methanol at 40°C for 3 h. After repeating the filtration two more times and the extraction is complete, the filtrate was concentrated under reduced pressure to obtain 1.67 g of the AJ extract. The extract solution was stored at -20°C.

Cell culture and treatment – The human kidney cortex proximal tubule epithelial cell line (HK-2) was obtained from the Korean Cell Line Bank (Seoul, Korea). The cells were cultured in Dulbecco's modified Eagle medium with 1 g/L glucose (DMEM; Gibco, NY, USA) supplemented with 10% fetal bovine serum (FBS; Gibco) and 1% penicillin-streptomycin (P/S; Gibco). The cells were grown

at 37°C in a 5% CO₂ humidified incubator with medium changes every 48 h.

To assess the acute kidney injury model *in vitro*, cells were seeded at a density of 3×10^5 cells/well in 6-well plates (SPL, Pocheon, Korea) followed by treatment with 20 µM cisplatin (Sigma-Aldrich, MO, USA) for 24 h. The AJ extract (50 and 100 µg/mL) was added 6 h before harvest. The cells were washed in phosphate buffered saline (PBS) and collected for further analysis.

Cell viability assay – HK-2 cells (5×10^3 cells/well) were seeded in 96-well plates with growth media (DMEM supplemented with 10% FBS and 1% P/S) and incubated for 24 h. After 24 h, the cells were treated with AJ (0, 10, 50, and 100 µg/mL) and incubated for 24 h. For cell viability evaluation, the 3-(4,5-dimethylthiazol-2-yl)-2,5-diphenyltetrazolium bromide (MTT) assay was performed using the EZ-Cytox Cell Viability Assay Kit (Daeil, Korea) according to the manufacturer's instructions.

Annexin V staining – HK-2 cells were seeded in a 6-well plate at a density of (5×10^3 cells/well) for 24 h in a 5% CO₂ humidified incubator at 37°C. After 24 h, the cells were treated with 20 µM cisplatin (Sigma Aldrich) and AJ (50 and 100 µg/mL) for 6 h before harvest. The cells were stained with FITC annexin V and propidium iodide (PI; BioLegend, CA, USA) and analyzed by flow cytometry (BD Bioscience, NJ, USA). Apoptosis was expressed as the percentage of late apoptotic cells.

AKI animal model – Animal experiments were approved by the Institutional Animal Ethics Committee of Chungnam National University (202206-CNU-107). Twenty-four eight-week-old male C57BL/6 mice were obtained from Orient Bio (Seongnam, Korea). Before the experiments, the mice were acclimated under stable conditions ($25 \pm 0.2^\circ\text{C}$, $55 \pm 5\%$ humidity, and 12 h light/dark cycle) at a specific-pathogen-free animal facility for one week. All mice were cared for according to the principles of the Care and Use of Laboratory Animals of the National Institutes of Health.

One week after acclimation, the mice were randomly divided into four groups (n = 6): (1) NC (negative control), (2) AKI (cisplatin 25 mg/kg), (3) AJ 50 (cisplatin 25 mg/kg + AJ 50 mg/kg), and (4) AJ 100 (cisplatin 25 mg/kg + AJ 100 mg/kg). Cisplatin and AJ were dissolved in normal saline and PBS, respectively. AJ was orally administered to the mice once daily for ten consecutive days at doses of 50 and 100 mg/kg. On test day 8, cisplatin (25 mg/kg) was intraperitoneally (I.P.) injected into the mice 3 h before AJ treatment. Seventy-two hours after cisplatin injection, the mice were sacrificed. Serum and kidney tissue samples were obtained.

Serum chemistry – Blood urea nitrogen (BUN) and serum creatinine (CRE) levels were measured to evaluate kidney injury in mice. The obtained mouse serum was separated by centrifugation at 12,000 rpm for 15 min at 4°C and analyzed using a dry chemistry analyzer (Fujifilm, Tokyo, Japan).

Histological study – Kidney tissues were collected and fixed immediately with 10% buffered formalin phosphate solution (Sigma-Aldrich) and embedded in paraffin. Paraffin-embedded kidneys were cut into 5- μ m-thick sections, deparaffinized, and dehydrated. Kidney tissue was stained with hematoxylin and eosin. Ten randomly selected areas on each slide were evaluated using a light microscope (Nikon ECLIPSE Ni-U, Tokyo, Japan).

For immunohistochemistry, deparaffinized and dehydrated kidney sections were treated with 3% quenched endogenous peroxidase (SAMCHUN Chemicals, Pyongtack, Korea) and 0.5% Triton X-100 (Sigma-Aldrich) for 30 min. Non-specific binding was blocked with normal goat serum (Vector Labs, Burlingame, CA, USA) for 2 h. The blocked specimens were then incubated with primary anti-neutrophil gelatinase-associated lipocalin (NGAL; 1:200, ABclonal, MA, USA) overnight at 4°C. One day later, the sections were incubated with secondary goat anti-rabbit antibody (1:200; AbFrontier, Seoul, Korea) for 2 h. Then, 4',6-diamidino-2-phenylindole (DAPI; Vector Labs) was used to mount the sections, and the stained cells were detected as green fluorescence under a microscope (Nikon ECLIPSE Ni-U). Ten randomly selected areas on each slide were assessed using a light microscope (Nikon ECLIPSE Ni-U). Immunofluorescence intensity was quantified using Image J software (Image J v46a, USA).

TUNEL assay – Deparaffinized and dehydrated sections were incubated with proteinase K and 3% quenched endogenous peroxidase (SAMCHUN Chemicals). After washing with distilled water, the sections were treated with equilibration buffer and TdT enzyme (EMD Millipore Corporation). Apoptosis detection was performed according to the manufacturer's protocol (*ApopTag*[®] Peroxidase In situ Apoptosis Detection Kit; EMD Millipore Corporation). Mayer's hematoxylin (Dako, Carpinteria, USA) was used to mount the sections, and dead cells were detected using 3,3-diaminobenzidine (Vector Labs). Images were randomly captured in ten areas using a microscope (Nikon ECLIPSE Ni-U) at 400X magnification. The number of dead cells was counted using Image J software (Image J v46a).

Western blot – The cells and kidney tissue were lysed in a radio-immunoprecipitation assay buffer (Cell Signaling Technology, MA, USA) and centrifuged at 12,000 rpm

for 15 min at 4°C. The protein concentration of the collected supernatant was determined using a bicinchoninic acid assay. Equal quantities of protein samples were separated by 8-12% sodium dodecyl sulfate polyacrylamide gel electrophoresis and transferred onto polyvinylidene fluoride membranes using a wet transfer system (Bio-Rad, CA, USA). The membranes were blocked with 5% skim milk for 2 h and incubated with the following primary antibodies at 4°C for overnight: anti- β -actin (1:5000; Abcam, Cambridge, UK), anti-Bcl-2 associated X (Bax; 1:400; Santa Cruz, Texas, USA), anti-B cell lymphoma 2 (Bcl-2; 1:400; Santa Cruz), anti-kidney injury molecule-1 (KIM-1; 1:1000; ABclonal), anti-phospho-AMP-activated kinase (p-AMPK; 1:1000; Cell Signaling), anti-AMP-activated kinase (AMPK; 1:1000; Cell Signaling), anti-Dynamin-related protein-1 (Drp-1; 1:1000; Novus Biologicals, CO, USA), anti-mitochondrial fission factor (MFF; 1:1000; Santa Cruz), and anti-Caspase3 (1:1000; Cell Signaling). After incubation with the primary antibodies, the membranes were incubated with horseradish peroxidase-conjugated IgG secondary antibodies (anti-rabbit or anti-mouse; 1:5000; AbFrontier). Protein expression was detected using an enhanced chemiluminescence detection kit (Bio-Rad) and quantified using the CS Analyzer 4 program (Atto, Tokyo, Japan).

Statistical analysis – Data are expressed as mean \pm standard deviation (SD). All statistical analyses were performed by one-way analysis of variance with a Tukey's method using Sigmaplot 12.0. Statistical significance was set at $p < 0.05$.

Results and Discussion

In cisplatin-induced AKI, cellular accumulation of cisplatin is mediated by a variety of transporters located in renal proximal tubule epithelial cells. Therefore, the renal proximal tubule is considered the main target of cisplatin-induced AKI.¹¹ Therefore, the human proximal tubule epithelial cell line HK-2 was used to examine the effects of AJ *in vitro*. At the beginning of the study, the cytotoxicity of AJ extract on HK-2 cells was investigated using an MTT assay. As the concentration of AJ increased (10, 50, and 100 μ g/mL), cell viability increased in a dose-dependent manner, suggesting there is no cytotoxicity to HK-2 cells (Fig. 1A). In addition, cisplatin treatment reduced the cell viability of HK-2 cells compared to that of control group. However, the cell viability of HK-2 cells co-treated with cisplatin and AJ (50 and 100 μ g/mL) increased to a similar level to that of the control group (Fig. 1B). Cisplatin treatment induces apoptosis in renal

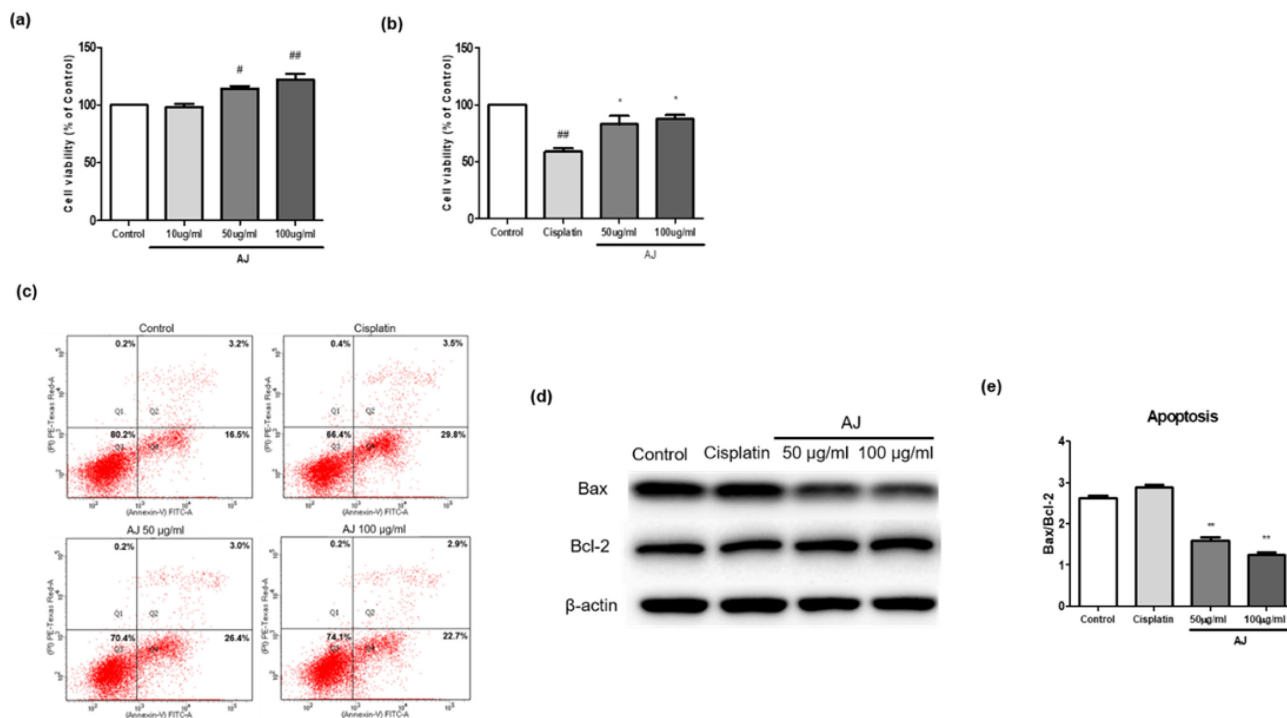


Fig 1. Effects of AJ in apoptosis on cisplatin-treated HK-2 cells. (a) Cell viability (b) HK-2 cells were incubated without (Control)/with cisplatin (25 μ M) alone or cisplatin (25 μ M) with AJ (50 or 100 μ g/ml). (c) The cells were stained with annexin-V-FITC and PI. The identification of apoptotic cells was conducted by the flow cytometry. (d) Western blot analysis of Bcl-2 and Bax expression levels. (e) Apoptosis was quantified as the ratio of Bax to Bcl-2. Values are expressed as the mean \pm SEM. Significant differences were determined compared with Control group ([#] $p < 0.05$; ^{##} $p < 0.01$) and Cisplatin group (^{*} $p < 0.05$; ^{**} $p < 0.01$).

proximal tubule epithelial cells, which is a representative pathological characteristic of AKI.¹⁵ Cellular absorbed cisplatin disturbs DNA repair mechanisms and inhibits the production of DNA replication templates, leading to cell death.¹⁰ The anti-apoptotic activity of AJ was investigated to evaluate its effects on cisplatin-induced AKI. We performed annexin V staining to detect the degree of apoptotic cells treated with AJ on cisplatin-treated HK-2 cells. The number of cells undergoing early (Q1) and late (Q4) apoptosis in cisplatin-treated HK-2 cells was higher than that in control HK-2 cells. However, the number of apoptotic cells in AJ-treated HK-2 cells was lower than that in cisplatin-treated HK-2 cells (Fig. 1B). The ratio of Bax to Bcl-2 (Bax/Bcl-2), an indicator of apoptosis, increased in cisplatin-treated HK-2 cells compared to that in control HK-2 cells. AJ treatment decreased the level of Bax/Bcl-2 in a dose-dependent manner compared to that in cisplatin-treated HK-2 cells (Fig. 1C). Collectively, AJ treatment downregulated cisplatin-induced apoptosis of HK-2 cells *in vitro*.

Based on *in vitro* results, the therapeutic effects of AJ were examined in an *in vivo* animal study using a cisplatin-induced AKI mouse model. Once cisplatin enters

the cell and is activated, severe renal function damage is accompanied by cisplatin-induced nephrotoxicity.¹¹ In the present study, the AKI group showed a significant ($p < 0.01$) increase in the serum levels of BUN and CRE compared with the NC group. However, AJ treatment decreased the serum levels of BUN in a dose-dependent manner compared with the AKI group. Additionally, AJ treatment significantly ($p < 0.05$) decreased CRE level compared to the NC group (Fig. 2A). To assess the effect of AJ on cisplatin-induced AKI, we evaluated the expression levels of KIM-1 and NGAL, which are renal tubular injury markers. KIM-1 is a novel marker for the diagnosis of AKI, with a high expression level in the proximal tubule epithelial cells of AKI patients.¹⁹ Our results showed that the KIM-1 levels were significantly ($p < 0.05$) higher in the AKI group than in the NC group. However, the expression level of KIM-1 was significantly ($p < 0.01$) decreased with AJ treatment in comparison to the AKI group in a dose-dependent manner (Fig. 2B). NGAL level were upregulated in AKI and suggested to be an early predictor of AKI in both experimental and clinical studies.²⁰ In our study, immunofluorescence localization of NGAL was detected in the cytoplasm of

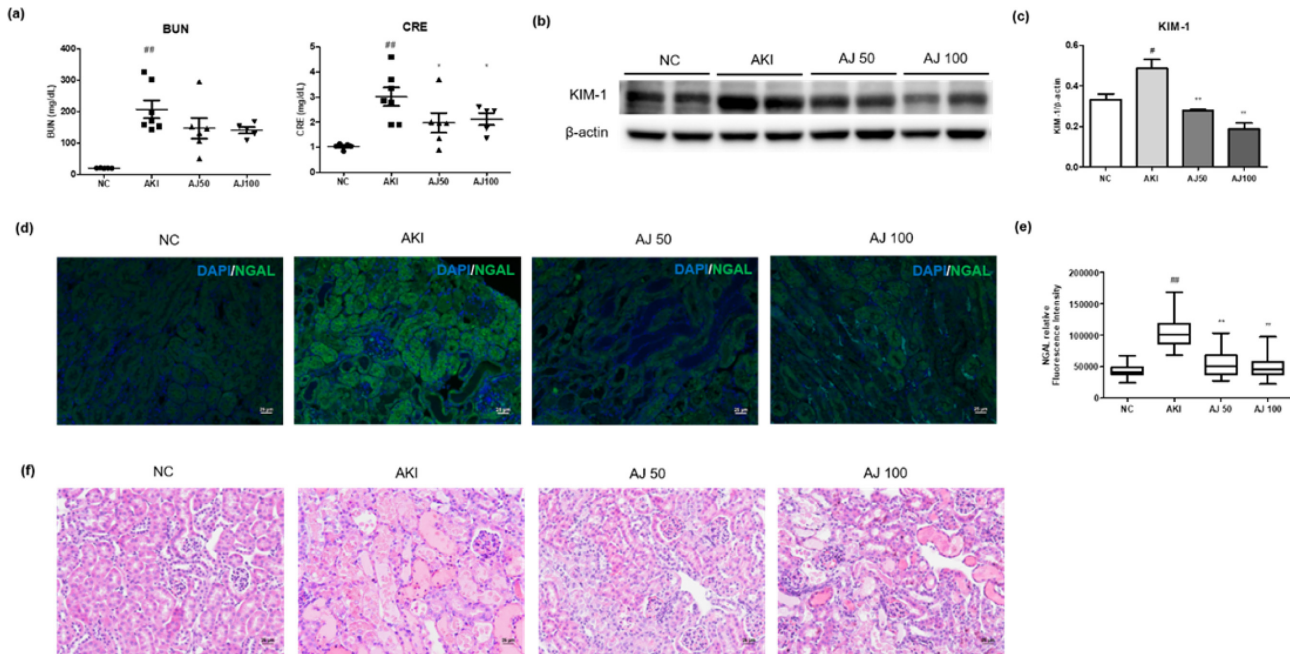


Fig 2. Effects of AJ in renal function on cisplatin-induced AKI mouse models. (a) The level of BUN and CRE in mice serum (b) Western blot analysis of KIM-1 expression level. (c) Band intensity of KIM-1 was normalized to that of β -actin. (d) The kidney tissues of mice were stained via immunofluorescence. NGAL was tagged by FIFC (green). Scale bar = 25 μ m. (e) Quantification of immunofluorescence stained area of NGAL. (f) Histopathological images of mice kidney tissues. Scale bar = 25 μ m. Values are expressed as the mean \pm SEM. Significant differences were determined compared with NC group ([#] $p < 0.05$; ^{##} $p < 0.01$) and AKI group (^{*} $p < 0.05$; ^{**} $p < 0.01$). Abbreviation: NC (normal saline P.O.), AKI (25 mg/kg cisplatin, I.P. + normal saline P.O.), AJ 50 (25 mg/kg cisplatin, I.P. + AJ 50 mg/kg P.O.), and AJ 100 (25 mg/kg cisplatin, I.P. + AJ 100 mg/kg P.O.)

proximal tubule cells in the cortex. The staining intensity of NGAL was significantly ($p < 0.01$) higher in the AKI group than in the NC group, whereas AJ treatment significantly ($p < 0.01$) decreased the staining intensity of NGAL (Fig. 2C). In the histopathological study, cisplatin treatment resulted in tubular epithelial cell loss, brush border desquamation and a large number of cell fragments within the tubular lumen compared with the NC group. However, in the AJ-treated groups, these histopathological alterations were markedly improved compared with those in the AKI group, showing reduced tubular loss and cell fragments (Fig. 2D). These results suggest that AJ treatment recovers renal function and tubular cell injury in cisplatin-induced AKI mouse models.

To determine the effect of AJ on mitochondrial fission, we studied the expression levels of mitochondrial fission related proteins such as AMPK, DRP-1, and MFF. AMPK, a major sensor of energy stress, detects energy depletion and promotes mitochondrial fission.²¹⁻²² It has been reported that the phosphorylation of AMPK decreased in the renal tissue of cisplatin-treated AKI mice compared that in the control mice.²³ Consistent with a previous report, our results showed that cisplatin treatment reduced

the phosphorylation level of AMPK, whereas AJ treatment significantly ($p < 0.01$) increased the phosphorylation of AMPK in comparison to the AKI group. DRP-1 is a critical protein for mitochondrial fission, accumulating in the outer mitochondrial membrane by binding to the MFF and mediating mitochondrial scission.²⁴ The expression of DRP-1 increased in AKI-induced renal tissue.^{23,25} In our study, the expression of DRP-1 was more than a threefold higher in the AKI group than in the NC group ($p < 0.01$). However, AJ treatment significantly ($p < 0.01$) decreased the expression of DRP-1 compared to that in AKI group. Concomitant with increased DRP-1 expression, MFF expression levels were dramatically increased ($p < 0.01$) in the AKI group compared to the NC group, whereas AJ treatment significantly ($p < 0.01$) reduced the expression level of MFF compared to the NC group (Fig 3A and B). Collectively, these results indicate that AJ treatment prevents the cisplatin-induced mitochondrial fission in an AKI mouse model.

Associated with mitochondrial fission, we examined the anti-apoptotic effects of AJ in a cisplatin-induced AKI mouse model. In the present study, the number of TUNEL-positive cells was two-fold higher in the AKI

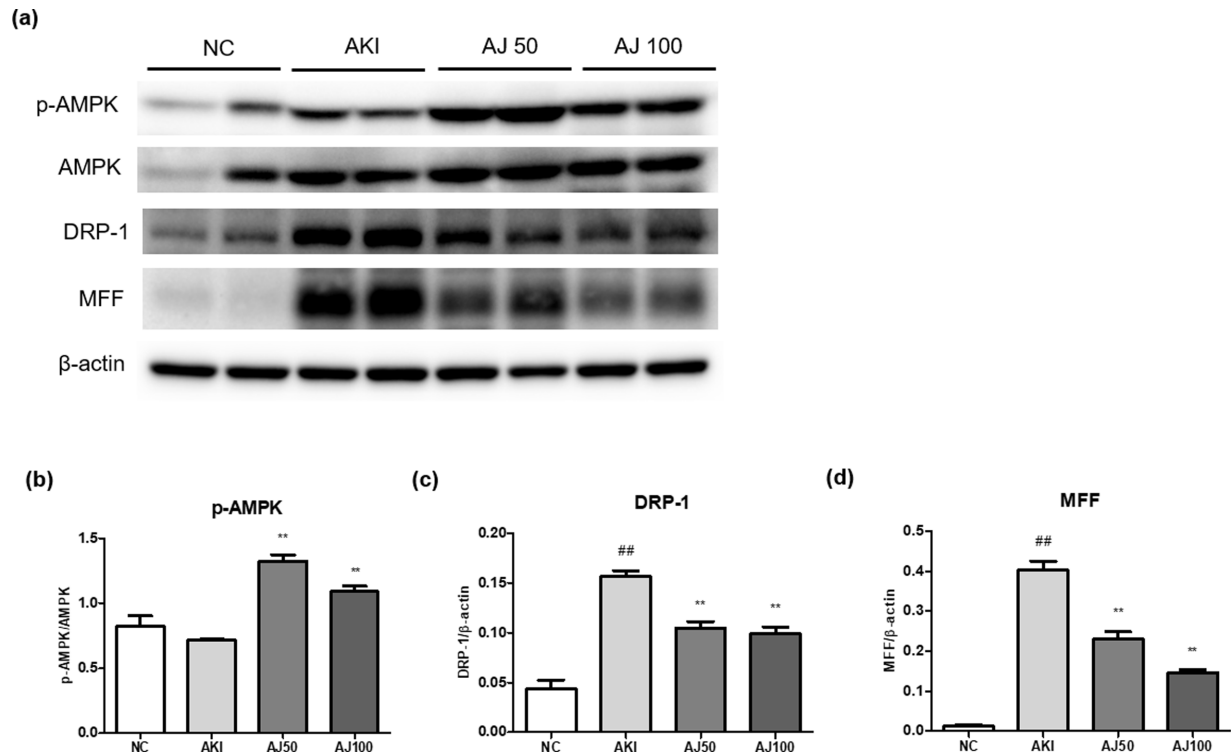


Fig 3. Effects of AJ in mitochondrial fission on cisplatin-induced AKI mouse models. (a) Western blot analysis of p-AMPK, AMPK, DRP-1, and MFF expression levels. (b) Band intensity of p-AMPK was quantified as the ratio of p-AMPK and AMPK (c) Band intensity of DRP-1 was normalized to that of β-actin. (d) Band intensity of MFF was normalized to that of β-actin. Values are expressed as the mean ± SEM. Significant differences were determined compared with NC group (* $p < 0.05$; ## $p < 0.01$) and AKI group (* $p < 0.05$; ** $p < 0.01$). Abbreviation: NC (normal saline P.O.), AKI (25 mg/kg cisplatin, I.P. + normal saline P.O.), AJ 50 (25 mg/kg cisplatin, I.P. + AJ 50 mg/kg P.O.), and AJ 100 (25 mg/kg cisplatin, I.P. + AJ 100 mg/kg P.O.)

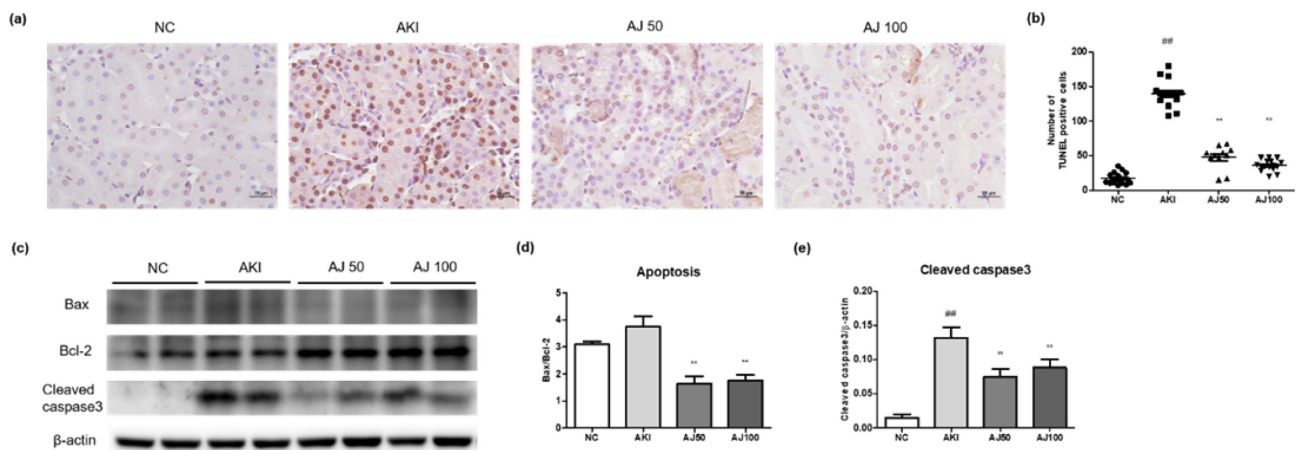


Fig 4. Effects of AJ in apoptosis on cisplatin-induced AKI mouse models. (a) TUNEL staining images of mice kidney tissues. Scale bar = 25 μm. (b) Quantification of TUNEL positive cells. (c) Western blot analysis of Bax, Bcl-2, and cleaved caspase3 expression levels. (d) Apoptosis was quantified as the ratio of Bcl-2 and Bax. (e) Band intensity of cleaved caspase3 was normalized to that of β-actin. Values are expressed as the mean ± SEM. Significant differences were determined compared with NC group (* $p < 0.05$; ## $p < 0.01$) and AKI group (* $p < 0.05$; ** $p < 0.01$). Abbreviation: NC (normal saline P.O.), AKI (25 mg/kg cisplatin, I.P. + normal saline P.O.), AJ 50 (25 mg/kg cisplatin, I.P. + AJ 50 mg/kg P.O.), and AJ 100 (25 mg/kg cisplatin, I.P. + AJ 100 mg/kg P.O.)

group than that in the NC group. However, AJ treatment decreased the number of TUNEL-positive cells compared

to that in AKI group (Fig 4A and B). Additionally, we examined the expression levels of apoptotic protein

markers. The level of Bax/Bcl-2 was significantly higher in the AKI group than in the NC group, whereas AJ treatment significantly ($p < 0.01$) reduced the level of Bax/Bcl-2 in comparison with the AKI group. Cleaved caspase3, a mediator of apoptosis, significantly ($p < 0.01$) increased in the AKI group compared to that in the NC group. However, the expression of cleaved caspase3 was lower in the AJ-treated groups than in the AKI group. These changes indicate that AJ treatment alleviated cisplatin-induced apoptosis in AKI mouse models. In accordance with Kwon et al., 3',4',7-Trihydroxyflavone, which is a flavonoid glycoside found in AJ, inhibited apoptotic cell death induced by mitochondrial dysfunction⁶. We suggest that 3',4',7-Trihydroxyflavone is a potential chemical component for alleviating cisplatin-induced AKI. Further studies are needed to elucidate the phytoconstituents of AJ that play a protective role in cisplatin-induced AKI.

In conclusion, we found that AJ significantly inhibited cisplatin-induced AKI by suppressing loss of renal function, mitochondrial fission, and apoptosis. Therefore, our study suggests that AJ is an alternative and potential therapeutic agent to protect against cisplatin-induced AKI.

Acknowledgements

This study was carried out with the support of 'R&D Program for Forest Science Technology (Project No. 2022421A00-2233-AA02) provided by Korea Forest Service (Korea Forestry Promotion Institute).

References

- (1) Han, L.; Pan, G.; Wang, Y.; Song, X.; Gao, X.; Ma, B.; Kang, L. *J. Pharm. Biomed. Anal.* **2011**, *55*, 996-1009.
- (2) Li, W.; Yang, H. *J. Molecules* **2020**, *25*, 2065.
- (3) Chang, J. S.; Liu, H. P.; Cheng, J.; Chen, C. J.; Hwang, S. L.; Tseng, C. C.; Hsu, L. F.; Lin, W. Y. *Evid. Based Complement. Alternat. Med.* **2019**, *2019*, 7395962.
- (4) Kokila, K.; Priyadharshini, S. D.; Sujatha, V. *Int. J. Pharm. Pharm. Sci.* **2013**, *5*, 70-73.
- (5) Zheng, L.; Zheng, J.; Zhao, Y.; Wang, B.; Wu, L.; Liang, H. *Bioorg. Med. Chem. Lett.* **2006**, *16*, 2765-2768.
- (6) Kwon, S. H.; Hong, S. I.; Ma, S. X.; Lee, S. Y.; Jang, C. G. *Food Chem. Toxicol.* **2015**, *80*, 41-51.
- (7) Gupta, A.; Mishra, A. K.; Bansal, P.; Kumar, S.; Sannd, R.; Gupta, V.; Goyal, B. M.; Singh, A. K.; Kumar, A. *Drug Invent. Today* **2010**, *2*, 191-193.
- (8) Zuk, A.; Bonventre, J. V. *Annu. Rev. Med.* **2016**, *67*, 293-307.
- (9) Yuan, L.; Yuan, Y.; Liu, F.; Li, L.; Liu, J.; Chen, Y.; Cheng, J.; Lu, Y. *Aging* **2021**, *13*, 8421-8439.
- (10) McSweeney, K. R.; Gadanec, L. K.; Qaradakh, T.; Ali, B. A.; Zulli, A.; Apostolopoulos, V. *Cancers (Basel)* **2021**, *13*, 1572.
- (11) Kuhlmann, M. K.; Burkhardt, G.; Köhler, H. *Nephrol. Dial. Transplant.* **1997**, *12*, 2478-2480.
- (12) Bhargava, P.; Schnellmann, R. G. *Nat. Rev. Nephrol.* **2017**, *13*, 629-646.
- (13) Kleele, T.; Rey, T.; Winter, J.; Zaganelli, S.; Mahecic, D.; Perreten Lambert, H.; Ruberto, F. P.; Nemir, M.; Wai, T.; Pedrazzini, T.; Manley, S. *Nature* **2021**, *593*, 435-439.
- (14) Zhang, X.; Agborbesong, E.; Li, X. *Int. J. Mol. Sci.* **2021**, *22*, 11253.
- (15) Wang, J.; Pabla, N.; Wang, C. Y.; Wang, W.; Schoenlein, P. V.; Dong, Z. *Am. J. Physiol. Renal Physiol.* **2006**, *291*, F1300-F1307.
- (16) Wang, Y.; Cai, J.; Tang, C.; Dong, Z. *Cells* **2020**, *9*, 338.
- (17) Rosner, M. H.; Perazella, M. A. *Kidney Res. Clin. Pract.* **2019**, *38*, 295-308.
- (18) Hong, G. L.; Kim, H. T.; Park, S. R.; Lee, N. H.; Ryu, K. A.; Kim, T. W.; Song, G. Y.; Jung, J. Y. *Nat. Prod. Sci.* **2019**, *25*, 200-207.
- (19) Tanase, D. M.; Gosav, E. M.; Radu, S.; Costea, C. F.; Ciocoiu, M.; Caraulleanu, A.; Lacatusu, C. M.; Floria, M.; Rezus, C. *Int. J. Mol. Sci.* **2019**, *20*, 5238.
- (20) Törnblom, S.; Nisula, S.; Petäjä, L.; Vaara, S. T.; Haapio, M.; Pesonen, E.; Pettile, V.; FINNAKI study group. *Ann. Intensive Care* **2020**, *10*, 51.
- (21) Shaw, R. J.; Kosmatka, M.; Bardeesy, N.; Hurley, R. L.; Witters, L. A.; DePinto, R. A.; Cantley, L. C. *Proc. Natl. Acad. Sci. U S A.* **2004**, *101*, 3329-3335.
- (22) Toyama, E. Q.; Herzig, S.; Courchet, J.; Lewis, T. L. Jr.; Losón, O. C.; Hellberg, K.; Young, N. P.; Chen, H.; Polleux, F.; Chen, D. C.; Shaw, R. J. *Science* **2016**, *351*, 275-281.
- (23) Morigi, M.; Perico, L.; Rota, C.; Longaretti, L.; Conti, S.; Rottoli, D.; Novelli, R.; Remuzzi, G.; Benigni, A. *J. Clin. Invest.* **2015**, *125*, 715-726.
- (24) Labbé, K.; Murley, A.; Nunnari, J. *Annu. Rev. Cell Dev. Biol.* **2014**, *30*, 357-391.
- (25) Zhao, C.; Chen, Z.; Qi, J.; Duan, S.; Huang, Z.; Zhang, C.; Wu, L.; Zeng, M.; Zhang, B.; Wang, N.; Mao, H.; Zhang, A.; Xing, C.; Yuan, Y. *Oncotarget* **2017**, *8*, 20988-21000.

Received October 25, 2022
 Revised November 25, 2022
 Accepted December 14, 2022